IEEE Access
Multidisciplinary | Rapid Review | Open Access Journal

Received November 24, 2019, accepted December 10, 2019, date of publication December 18, 2019,
date of current version December 30, 2019.

Digital Object Identifier 10.1109/ACCESS.2019.2960572

An Efficient Index Mapping Algorithm for OFDM-Index Modulation

EUNCHUL YOON[1], (Senior Member, IEEE), SUN-YONG KIM[1], (Senior Member, IEEE), SOONBUM KWON[1], AND UNIL YUN[2]

[1]Department of Electrical and Electronics Engineering, Konkuk University, Seoul 05029, South Korea
[2]Department of Computer Engineering, Sejong University, Seoul 05006, South Korea

Corresponding author: Unil Yun (yunei@sejong.ac.kr)

This work was supported by Konkuk University in 2017.

ABSTRACT An index mapping algorithm that efficiently associates the subcarrier activation pattern (SAP) or constellation mode pattern (CMP) sequences with the index selecting bit (ISB) sequences is proposed to improve the error performances of two OFDM-'index modulation' (IM) variants, OFDM-'in-phase/quadrature' (IQ)-IM and 'coordinate interleaving' (CI)-'multiple-mode' (MM)-OFDM-IM. If the Hamming distances between every combinational pair of the Gray-coded ISB sequences are written in a 2-dimensional Hamming distance table, the minimum Hamming distances (i.e., 1's) are located in an X-shaped cross. In the proposed index mapping algorithm, the selection and ordering of the SAP or CMP sequences is determined by a mapping strategy of locating the minimum Hamming distances (i.e., 2's) of the SAP or CMP sequences in the same X-shaped cross as that of the minimum Hamming distances (i.e., 1's) of the Gray-coded ISB sequences. A pseudo-code is provided to reify the proposed index mapping algorithm. We show by numerical simulation that the proposed index mapping algorithm can provide substantial performance improvement for various IM schemes such as OFDM-IQ-IM, CI-MM-OFDM-IM, and OFDM-IM, especially when an error correction code is applied simultaneously.

INDEX TERMS Communication system signaling, modulation, wireless communication.

I. INTRODUCTION

Index modulation (IM) is a promising technique for 5G and beyond wireless networks to achieve extra data rate by using the indices of the active resources, where the resources can be any transmission entities such as transmit antennas, subcarriers, modulation types, precoders, time slots, channel states and so on. Spatial modulation (SM) is another prospective technique that considers IM for the transmit antennas of a multiple-input multiple-output system. For an overview of SM and IM related literatures, interested readers are referred to [1] and the references therein. A comprehensive overview of the latest results and progresses in SM research were presented in [2]. A comprehensive overview of the latest existing IM schemes and their principles were presented in [3]. In IM, the status of resources is set to either active or inactive and the indices of the active resources are used as an additional dimension to convey the information. In [4], the idea of IM was merged with orthogonal frequency division multiplexing (OFDM) systems to come up with the subcarrier index modulation OFDM scheme (named SIM therein and OFDM-IM in other literatures). Since then, numerous OFDM-IM variants have been suggested [5]. OFDM-IM conveys extra information bits besides those transmitted by the data symbols, which can achieve an increased spectral efficiency (SE) and a superior bit error rate (BER) performance with a low modulation order when compared to classical OFDM [1]. In [6], the diversity order of OFDM-IM was derived analytically and the combinatorial method was suggested for one-to-one mapping between natural numbers and active subcarrier combinations. In [7], the OFDM scheme with generalized IM (OFDM-GIM) varied the number of active subcarriers according to the information bits for a higher SE. In [8], OFDM-IM was applied independently to the in-phase/quadrature (IQ) components of each subcarrier symbol, which was termed OFDM-GIM2 therein and OFDM-IQ-IM in other literatures (e.g., [9] and [10]). In [11], the dual mode OFDM-IM scheme (DM-OFDM-IM) employed two symbol constellation modes to transmit different modulation symbols not only over the active

The associate editor coordinating the review of this manuscript and approving it for publication was Prakasam Periasamy.

subcarriers but also over the inactive subcarriers. In [12], the generalized DM-OFDM-IM scheme (GDM-OFDM-IM) varied the number of subcarriers modulated by the same constellation alphabet according to the information bits to further improve the SE of DM-OFDM-IM. In [13], the scheme of multiple-mode OFDM-IM (MM-OFDM-IM) and the scheme of multiple-mode OFDM-IQ-IM (MM-OFDM-IQ-IM) were proposed, where the full permutation of symbol constellation modes were adopted according to the information bits. In [14], the scheme of layered OFDM-IM (L-OFDM-IM) was proposed, where the subcarriers in each subblock are divided into multiple layers and the active subcarriers and their modulated symbols were determined separately in each layer to increase the index bits. In order to improve the BER performance of OFDM-IM, numerous techniques have been developed. In [15], subcarrier level interleaving was introduced to improve the BER performance of OFDM-IM by benefiting from uncorrelated frequency-domain fading coefficients. In [16], the CI-OFDM-IM (CI-OFDM-IM) applied interleaving to the real and imaginary parts of every two complex symbols to obtain additional diversity gains. In [17], the scheme of enhanced CI-OFDM-IM (ECI-OFDM-IM) was proposed, where the subcarrier activation pattern (SAP) sequences with a minimum Hamming distance greater than or equal to 4 were used for CI-OFDM-IM to enhance the BER performance of the index bits. In [14], the scheme of CI-L-OFDM-IM was proposed to enhance diversity performance of L-OFDM-IM by using the CI technique. In [9], the linear constellation precoding (LCP) technique was applied to OFDM-IQ-IM, which was termed LCP-OFDM-IQ-IM. Inspired by [9] and [16], the coordinate interleaving was applied to MM-OFDM-IM and the LCP technique was applied to MM-OFDM-IQ-IM in [10], which were termed CI-MM-OFDM-IM and LCP-MM-OFDM-IQ-IM, respectively. In [18], the scheme of generalized MM-OFDM-IM (GMM-OFDM-IM) was proposed, where different subcarriers in a subblock used different signal constellation achieving better BER performance in the high SNR region. In [19], an equiprobable subcarrier activation approach was suggested, where all the OFDM-IM subcarriers were rendered to have equal chance of activation to improve SNR gain over the combinatorial method [6]. However, the equiprobable subcarrier activation approach could attain a significant SNR gain only for specific numbers of active subcarriers given a subblock. Moreover, it attained no gain for higher symbol modulation alphabets such as 16 phase shift keying (PSK) modulation. In [20] and [21], the lexicographic codebook design for OFDM-IM was introduced, where the SAP sequences were selected by using the channel state information (CSI). Since the lexicographic codebook requires closed-loop control over wireless networks for CSI feedback and entails its redesign according to the updated CSI, its applications should be limited to very slowly faded channels. In [22], the Gray-order mapping that associated the Gray-ordered antenna activation order (ACO) sequences with the index selecting bit (ISB) sequences was suggested for a differential spatial modulation (DSM) system to eliminate the necessity of using a mapping table. However, since the Gray-order mapping itself could not improve the BER performance, it required an additional technique such as coordinate interleaving. In [23], a Gray-coded index mapping was introduced for efficient mapping between the constellation mode pattern (CMP) sequences and the ISB sequences in DM-OFDM-IM. The Gray-coded index mapping led to a better BER performance of the index bits because it associated a pair of similar ISB sequences with a pair of similar CMP sequences and a pair of more contrasting ISB sequences with a pair of more contrasting CMP sequences. However, the application of the Gray-coded index mapping was limited only to the cases of small subblock sizes such as 2 and 4.

The purpose of this paper is to extend the idea of an efficient index mapping in [23] for subblock sizes larger than 4 and to other OFDM-IM schemes. Note that a false detection of a desired SAP sequence by an OFDM-IM demodulator leads to a false detection of an ISB sequence because every ISB sequence is mapped to a separate SAP sequence in a one-to-one manner. To reduce the bit errors occurring due to falsely detected SAP sequences, every pair of the SAP sequences that have minimum Hamming distance 2 should be associated with a separate pair of the ISB sequences that have minimum Hamming distance 1 because the probability that the OFDM-IM demodulator detects a wrong SAP sequence instead of the desired SAP sequence becomes the highest when the desired SAP sequence is different from the falsely detected SAP sequence in only two active subcarrier positions. Likewise, to reduce the bit errors occurring due to falsely detected CMP sequences, every pair of the CMP sequences that have minimum Hamming distance 2 should be associated with a separate pair of the ISB sequences that have minimum Hamming distance 1. However, it is very difficult to associate every pair of the SAP or CMP sequences that have minimum Hamming distance 2 with a separate pair of the ISB sequences that have minimum Hamming distance 1 if the subblock size is large.

In this paper, an index mapping algorithm that efficiently associates the SAP or CMP sequences with the ISB sequences is proposed to improve the error performances of two OFDM-IM variants, OFDM-IQ-IM and CI-MM-OFDM-IM. If the Hamming distances between every combinational pair of the Gray-coded ISB sequences are written in a 2-dimensional (2D) Hamming distance table, the minimum Hamming distances (i.e., 1's) are located in an X-shaped cross. In the proposed index mapping algorithm, the selection and ordering of the SAP or CMP sequences is determined by a mapping strategy of locating the minimum Hamming distances (i.e., 2's) of the SAP or CMP sequences in the same X-shaped cross as that of the minimum Hamming distances (i.e., 1's) of the Gray-coded ISB sequences. A pseudo-code is provided to reify the proposed index mapping algorithm. We show by numerical simulation that the proposed index mapping algorithm can provide substantial performance improvement for various IM schemes such as OFDM-IQ-IM,

CI-MM-OFDM-IM, and OFDM-IM, especially when an error correction code is applied simultaneously.

The remainder of this paper is organized as follows. Section-II describes the system models for OFDM-IQ-IM and CP-MM-OFDM-IM, respectively. Section-III proposes a mapping algorithm which can be used to efficiently associate the ISB sequences not only with the SAP sequences in OFDM-IQ-IM, but also with the CMP sequences in CP-OFDM-MM-IM. Section-IV discusses several issues related with the proposed index mapping algorithm. Section-V presents simulation results to evaluate merits of the proposed index mapping algorithm and investigate the impact of an error correction code on the performance of the proposed index mapping algorithm. Section-VI provides with concluding remarks.

Notatons: $(\cdot)^T$ denotes the transpose operator. $\lfloor x \rfloor$ denotes the greatest integer less than or equal to its argument. $\Re(\cdot)$ and $\Im(\cdot)$ denote the real and imaginary parts of its argument, respectively. diag($\mathbf{x}$) denotes a diagonal matrix with its diagonal components given by a vector $\mathbf{x}$. $\oplus$ denotes the XOR operator. dist($\mathbf{x}_1, \mathbf{x}_2$) denotes the Hamming distance between $\mathbf{x}_1$ and $\mathbf{x}_2$ or the number of the non-zero components in $\mathbf{x}_1 - \mathbf{x}_2$, where $\mathbf{x}_1$ and $\mathbf{x}_2$ are two vectors of the same length. len($\mathbf{x}$) denotes the number of the components of a vector $\mathbf{x}$. $\mathbf{x}(i)$ denotes the i-th component of a vector $\mathbf{x}$ for $i = 1, 2, \cdots,$ len($\mathbf{x}$). $\mathcal{A} - \mathcal{B}$ denotes set difference defined by $\{x : x \in \mathcal{A}$ and $x \notin \mathcal{B}\}$.

II. SYSTEM MODEL

While our index mapping algorithm can be applied to various IM schemes, in order to emphasize the merits of our index mapping algorithm, we apply our index mapping algorithm to two OFDM-IM schemes, OFDM-IQ-IM and CP-MM-OFDM-IM, which are known to outperform classical OFDM in terms of BER performance. Firstly, in OFDM-IQ-IM, our index mapping algorithm is used to find the mapping between the ISB and SAP sequences. Secondly, in CP-MM-OFDM-IM, our index mapping algorithm is used to find the mapping between the ISB and CMP sequences. In the following, the system properties that are common to OFDM-IQ-IM and CP-MM-OFDM-IM are described first. Then, the system properties unique to each system are described in separate subsections.

Consider an OFDM system operating in a frequency-selective channel environment. The frequency-selective channel is modeled as a tapped delay-line of length ν, where the channel impulse response is given by

$$\mathbf{h} = [\, h_0 \; h_1 \; \cdots \; h_{\nu-1} \,]^T . \tag{1}$$

The channel coefficients $\{h_l\}_{l=0}^{\nu-1}$ are assumed to be uncorrelated with each other and have zero-mean circularly symmetric complex Gaussian distribution with $\mathcal{CN}(0, 1/\nu)$. We assume that the OFDM block consists of N subcarriers and conveys N_I information bits per OFDM block. In order to apply IM, the OFDM block is divided into N_B subblocks, where each subblock with $n = N/N_B$ subcarriers conveys $p = N_I/N_B$ information bits. The OFDM block comprising N_B subblocks can be written as

$$\mathbf{X} = \left[\, \mathbf{X}^{(1)^T} \; \mathbf{X}^{(2)^T} \; \cdots \; \mathbf{X}^{(N_B)^T} \,\right]^T, \tag{2}$$

where $\mathbf{X}^{(\beta)}$ denotes the β-th subblock,

$$\mathbf{X}^{(\beta)} = \left[\, X_1^{(\beta)} \; X_2^{(\beta)} \; \cdots \; X_n^{(\beta)} \,\right]^T. \tag{3}$$

Since subcarrier-level interleaving can improve the error performance by turning the frequency domain channel into a uncorrelated one ([15]), we assume that the OFDM block, $\mathbf{X}$, passes through a symbol-level interleaver to give

$$\mathbf{X}' = \left[\, X_1^{(1)} \cdots X_1^{(N_B)} \, X_2^{(1)} \cdots X_2^{(N_B)} \, X_n^{(1)} \cdots X_n^{(N_B)} \,\right]^T. \tag{4}$$

$\mathbf{X}'$ undergoes inverse fast Fourier transform and addition of the cyclic prefix of length L_c, before transmission. At the receiver, the processes of cyclic prefix elimination, fast Fourier transform, and de-interleaving are applied to the received signal. Then, the received signal for the β-th subblock, $\beta = 1, 2, \cdots, N_B$, can be written as

$$\mathbf{Y}^{(\beta)} = \mathrm{diag}\big(\mathbf{X}^{(\beta)}\big)\mathbf{H}^{(\beta)} + \mathbf{W}^{(\beta)}, \tag{5}$$

where $\mathbf{H}^{(\beta)}$ denotes the frequency domain channel vector,

$$\mathbf{H}^{(\beta)} = \left[\, H_1^{(\beta)} \; H_2^{(\beta)} \; \cdots \; H_n^{(\beta)} \,\right]^T, \tag{6}$$

with its component defined by

$$H_m^{(\beta)} = \sum_{l=0}^{\nu-1} h_l e^{-j\frac{2\pi}{N} \times l \times ((\beta-1)n+m-1))}. \tag{7}$$

$\mathbf{W}^{(\beta)}$ denotes an additive noise vector,

$$\mathbf{W}^{(\beta)} = \left[\, W_1^{(\beta)} \; W_2^{(\beta)} \; \cdots \; W_n^{(\beta)} \,\right]^T, \tag{8}$$

where $W_m^{(\beta)}$ has circularly symmetric complex Gaussian distribution with mean 0 and variance N_0. The signal-to-noise ratio (SNR) is defined as $\rho = E_b/N_0$, where $E_b = (N + L_c)/N_I$ denotes the average energy per bit. The spectral efficiency of the OFDM-IM scheme is given by $N_I/(N + L_c)$ [bits/s/Hz].

A. THE OFDM-IQ-IM SCHEME

The transmitter structure of OFDM-IQ-IM is depicted in Fig. 1 (a). The p bits given for a subblock are equally divided into p^I and p^Q bits and used for the in-phase ($I-$) and quadrature ($Q-$) branches, respectively. Due to the similarity of the modulation procedures on the $I-$ and $Q-$ branches, we focus on the $I-$branch in the following. With a subblock consisting of k active and $(n-k)$ inactive subcarriers, the total number of possible SAP candidate sequences is given by $N_{\mathrm{SAP}} = {}_nC_k$, where ${}_nC_k$ denotes the k-combinations from a set of n components. We represent an SAP sequence with a binary sequence consisting of k 1's and $(n-k)$ 0's, where 1 and 0 denote active and inactive subcarriers, respectively. The $\sqrt{M}$-ary pulse amplitude modulation (PAM) constellation is adopted by the $I-$branch of OFDM-IQ-IM for fair comparison in terms of SE with the classical

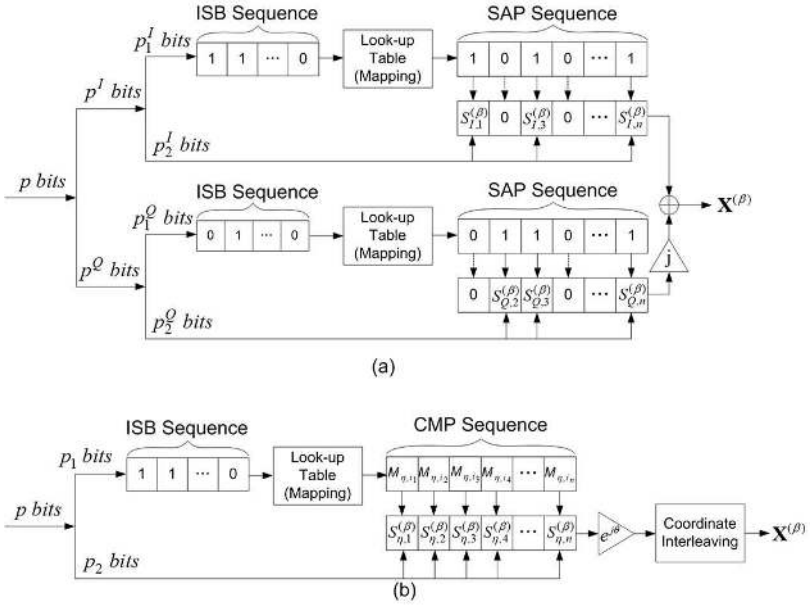

FIGURE 1. The transmitter structures of two OFDM-IM schemes: (a) OFDM-IQ-IM and (b) CI-MM-OFDM-IM.

OFDM that adopts the M-ary quadrature amplitude modulation (QAM) constellation. The p^I bits are separated into $p_1^I = \lfloor \log_2(N_{\text{SAP}}) \rfloor$ index bits and $p_2^I = k \log_2(\sqrt{M})$ data symbol bits. Since the $Q-$branch applies the same procedure as the $I-$branch, each subblock conveys total $p = 2\lfloor \log_2(N_{\text{SAP}}) \rfloor + k \log_2(M)$ information bits. An ISB sequence of length p_1^I is formed with p_1^I index bits. Each ISB sequence is associated with a separate SAP sequence,

$$\mathbf{SAP}_\eta = [\, b_{\eta,1}\ b_{\eta,2}\ \cdots\ b_{\eta,n}\,], \tag{9}$$

where $b_{\eta,m} \in \{0, 1\}$, $m = 1, 2, \cdots, n$, denotes the subcarrier activation bit and η denotes the SAP sequence index belonging to $\{1, 2, \cdots, 2^{p_1^I}\}$. For maximal SE, p_1^I is chosen as $p_1^I = \lfloor \log_2(N_{\text{SAP}}) \rfloor$. $2^{p_1^I}$ SAP sequences should be selected from N_{SAP} SAP candidate sequences because the SAP sequences are associated with the $2^{p_1^I}$ ISB sequences in a one-to-one manner. We assume that the information on the mapping between the ISB and SAP sequences is saved in a look-up table. According to $\mathbf{SAP}_\eta$, the data symbol vector for the $I-$branch of the β-th subblock is generated with the p_2^I data symbol bits as

$$\mathbf{S}_I^{(\beta)} = \left[\, \mathcal{S}_{I,\eta,1}^{(\beta)}\ \mathcal{S}_{I,\eta,2}^{(\beta)}\ \cdots\ \mathcal{S}_{I,\eta,n}^{(\beta)}\,\right], \tag{10}$$

where $\mathcal{S}_{I,\eta,m}^{(\beta)} \in \{0\} \cup \mathbb{S}$, $m = 1, 2, \cdots, n$, and $\mathbb{S}$ denotes the $\sqrt{M}$-ary PAM constellation. Note that a $\sqrt{M}$-ary PAM symbol is conveyed over the m-th subcarrier of a subblock only if the m-th component of $\mathbf{SAP}_\eta$ (i.e., $b_{\eta,m}$) is given by 1. Similarly to the above, the data symbol vector for the $Q-$branch of the β-th subblock is generated as $\mathbf{S}_Q^{(\beta)}$. Then, the β-th subblock, $\mathbf{X}^{(\beta)}$, $\beta = 1, 2, \cdots, N_B$, is determined as

$$\mathbf{X}^{(\beta)} = \mathbf{S}_I^{(\beta)} + j\mathbf{S}_Q^{(\beta)}. \tag{11}$$

At the OFDM-IQ-IM demodulator, the index of the SAP sequence for the $I-$branch of the β-th subblock can be found by using the maximum-likelihood (ML) method,

$$\hat{\eta} = \arg \min_{\eta} \sum_{m=1}^{n} \min_{\mathcal{S}_{I,\eta,m}^{(\beta)} \in \{0\} \cap \mathbb{S}} \left\| \Re\left(Y_m^{(\beta)}/H_m^{(\beta)}\right) - S_{I,\eta,m}^{(\beta)} \right\|^2. \tag{12}$$

One may refer to [8] for the log-likelihood ratio (LLR) detection method with reduced implementation complexity. Given the SAP sequence, the p_1^I index bits representing the ISB sequence can be retrieved by referring to the look-up table. Once the SAP sequence or equivalently, the SAP sequence index, $\hat{\eta}$, is estimated, the data symbol vector for the $I-$branch of the β-th subblock can be found by using the ML method,

$$\hat{\mathbf{S}}_I^{(\beta)} = \arg \min_{\mathbf{S}_I^{(\beta)}} \sum_{m=1}^{n} \left\| \Re\left(Y_m^{(\beta)}/H_m^{(\beta)}\right) - S_{I,\hat{\eta},m}^{(\beta)} \right\|^2. \tag{13}$$

The SAP sequence and the data symbol vector for the $Q-$branch can also be retrieved analogously. However, for the Q-branch, the $\Re(Y_m^{(\beta)}/H_m^{(\beta)})$ term, the $S_{I,\eta,m}^{(\beta)}$ term, and the $S_{I,\hat{\eta},m}^{(\beta)}$ term as shown in (12) and (13) should be replaced with $\Im(Y_m^{(\beta)}/H_m^{(\beta)})$, $S_{Q,\eta,m}^{(\beta)}$, $S_{Q,\hat{\eta},m}^{(\beta)}$, respectively.

B. THE CI-MM-OFDM-IM SCHEME

The transmitter structure of CI-MM-OFDM-IM is depicted in Fig. 1 (b). The incoming p bits are divided into p_1 index bits and p_2 data symbol bits. An ISB sequence of length p_1 is formed with p_1 index bits. Each ISB sequence is associated

with a separate CMP sequence,

$$\mathbf{CMP}_{\eta} = [\, M_{\eta,1}\, M_{\eta,2}\, \cdots\, M_{\eta,n}\,], \tag{14}$$

where $M_{\eta,m} \in \{1, 2, \cdots, n\}$, $m = 1, 2, \cdots, n$, denotes the symbol constellation mode and η denotes the CMP sequence index belonging to $\{1, 2, \cdots, 2^{p_1}\}$. The total number of possible CMP candidate sequences is given by $N_{\mathrm{CMP}} = n!$ (i.e., n factorial). For maximal SE, p_1 is chosen as $p_1 = \lfloor \log_2(N_{\mathrm{CMP}}) \rfloor$. 2^{p_1} CMP sequences should be selected from N_{CMP} CMP candidate sequences because the CMP sequences are associated with the 2^{p_1} ISB sequences in a one-to-one manner. We assume that the information on the mapping between the ISB and CMP sequences is saved in a look-up table. The n symbol constellations of CI-MM-OFDM-IM, $\mathcal{M}_{\eta,1}$, $\mathcal{M}_{\eta,2}$, $\cdots$, $\mathcal{M}_{\eta,n}$, can be prepared by partitioning the nM-ary PSK constellation as suggested in [10]. Each subblock conveys total $p = \lfloor \log_2(N_{\mathrm{CMP}}) \rfloor + n \log_2(M)$ information bits. According to $\mathbf{CMP}_{\eta}$, the data symbol vector for the β-th subblock is generated with the $p_2 = n \log_2(M)$ data symbol bits as

$$\mathbf{S}^{(\beta)} = \left[\, \mathcal{S}_{\eta,1}^{(\beta)}\, \mathcal{S}_{\eta,2}^{(\beta)}\, \cdots\, \mathcal{S}_{\eta,n}^{(\beta)} \,\right], \tag{15}$$

where $\mathcal{S}_{\eta,m}^{(\beta)} \in \mathcal{M}_{\eta,m}, m = 1, 2, \cdots, n$. Then, the data symbol vector $\mathbf{S}^{(\beta)}$ is multiplied by $e^{j\theta}$ to extract a CI effect. In [10], the optimal θ was derived analytically in terms of n and M. For n being an even number, the β-th subblock, $\mathbf{X}^{(\beta)}$, $\beta = 1, 2, \cdots, N_B$, is formed by applying the CI technique to every two symbols of $e^{j\theta}\mathbf{S}^{(\beta)}$ as

$$\mathbf{X}^{(\beta)} = \left[\, \mathbf{X}_1^{(\beta)T}\, \mathbf{X}_2^{(\beta)T}\, \cdots\, \mathbf{X}_{n/2}^{(\beta)T} \,\right]^T, \tag{16}$$

where

$$\mathbf{X}_k^{(\beta)} = \begin{bmatrix} X_{2k-1}^{(\beta)} \\ X_{2k}^{(\beta)} \end{bmatrix} = \begin{bmatrix} \Re\left(e^{j\theta}\mathcal{S}_{\eta,2k-1}^{(\beta)}\right) + j\Im\left(e^{j\theta}\mathcal{S}_{\eta,2k}^{(\beta)}\right) \\ \Re\left(e^{j\theta}\mathcal{S}_{\eta,2k}^{(\beta)}\right) + j\Im\left(e^{j\theta}\mathcal{S}_{\eta,2k-1}^{(\beta)}\right) \end{bmatrix} \tag{17}$$

for $k = 1, 2, \cdots, n/2$. At the CI-MM-OFDM-IM demodulator, the index of the CMP sequence can be found by using the ML method,

$$\hat{\eta} = \arg \min_{\eta} \sum_{k=1}^{n/2} \min_{\substack{S_{\eta,2k-1}^{(\beta)} \in \mathcal{M}_{\eta,2k-1} \\ S_{\eta,2k}^{(\beta)} \in \mathcal{M}_{\eta,2k}}} \left\| \mathbf{Y}_k^{(\beta)} - \mathrm{diag}\left(\mathbf{X}_k^{(\beta)}\right)\mathbf{H}_k^{(\beta)} \right\|^2, \tag{18}$$

where

$$\mathbf{Y}_k^{(\beta)} = \begin{bmatrix} Y_{2k-1}^{(\beta)} & Y_{2k}^{(\beta)} \end{bmatrix}^T, \tag{19}$$

and

$$\mathbf{H}_k^{(\beta)} = \begin{bmatrix} H_{2k-1}^{(\beta)} & H_{2k}^{(\beta)} \end{bmatrix}^T. \tag{20}$$

Given the CMP sequence, the p_1 index bits representing the ISB sequence can be retrieved by referring to the look-up table. Once the CMP sequence or equivalently, the CMP sequence index $\hat{\eta}$ is estimated, the data symbol vector for the β-th subblock can be found by using the ML method,

$$(\hat{S}_{2k-1}^{(\beta)}, \hat{S}_{2k}^{(\beta)}) = \arg \min_{\substack{S_{2k-1}^{(\beta)} \in \mathcal{M}_{\hat{\eta},2k-1} \\ S_{2k}^{(\beta)} \in \mathcal{M}_{\hat{\eta},2k}}} \left\| \mathbf{Y}_k^{(\beta)} - \mathrm{diag}\left(\mathbf{X}_k^{(\beta)}\right)\mathbf{H}_k^{(\beta)} \right\|^2 \tag{21}$$

for $k = 1, 2, \cdots, n/2$. One may refer to [10] for the ML methods with reduced implementation complexity.

III. PROPOSED INDEX MAPPING ALGORITHM

In this section, the proposed index mapping algorithm is explained for OFDM-IQ-IM first. Then, at the last part of this section, the proposed index mapping algorithm is explained for CI-MM-OFDM-IM.

A. INDEX MAPPING FOR OFDM-IQ-IM

Once again, we focus on the $I-$branch of the β-th subblock in OFDM-IQ-IM. For notational convenience, p_1^I is written as p_1 in the following. The i-th binary sequence of length p_1 for $i = 1, 2, \cdots, 2^{p_1}$ is defined as

$$\mathbf{B}_i = [\, b_{i,p_1}\, b_{i,p_1-1}\, \cdots\, b_{i,1}\,], \tag{22}$$

where $b_{i,l} \in \{0, 1\}$, $l = 1, 2, \cdots, p_1$. Note that b_{i,p_1} and $b_{i,1}$ represent the most significant bit (MSB) and the least significant bit (LSB) of $\mathbf{B}_i$, respectively. The i-th Gray-coded ISB sequence for $i = 1, 2, \cdots, 2^{p_1}$ is defined ([24]) as

$$\mathbf{ISB}_i = [\, d_{i,p_1}\, d_{i,p_1-1}\, \cdots\, d_{i,1}\,], \tag{23}$$

where

$$d_{i,l} = \begin{cases} b_{i,l} & \text{if } l = p_1 \\ b_{i,l} \oplus b_{i,l+1} & \text{if } l = 1, 2, \cdots, p_1 - 1. \end{cases} \tag{24}$$

The Hamming distance between two adjacent ISB sequences (i.e., $\mathbf{ISB}_i$ and $\mathbf{ISB}_{i+1}$ for $i = 1, 2, \cdots, p_1 - 1$) is always given by 1 due to the property of a Gray-code. It can be shown that the Hamming distance between $\mathbf{ISB}_i$ and $\mathbf{ISB}_{2^{p_1}-i+1}$ for $i = 1, 2, \cdots, 2^{p_1}$ is given by 1 (Refer to Appendix). Therefore, if the Hamming distances between every combinational pair of the Gray-coded ISB sequences are written in a 2D Hamming distance table, their minimum Hamming distances (i.e., 1's) are located in an X-shaped cross. In Fig. 2, the 2D Hamming distance table of $\{\mathbf{ISB}_i\}_{i=1}^{2^{p_1}}$ in the case of $p_1 = 4$ is presented. It can be seen that the minimum Hamming distances (i.e., 1's) of $\{\mathbf{ISB}_i\}_{i=1}^{2^{p_1}}$ are located in an X-shaped cross, which are highlighted in gray color. In order to associate as many pairs of the SAP sequences that have minimum Hamming distance 2 as possible with separate pairs of the Gray-coded ISB sequences that have minimum Hamming distance 1, we generate N_{SAP} SAP candidate sequences with k 1's and $(n-k)$ 0's, select 2^{p_1} sequences from those sequences, and then reorder the selected SAP candidate sequences according to a strategy of locating the minimum Hamming distances (i.e., 2's) of the 2^{p_1} SAP sequences in the same X-shaped cross as that of the minimum Hamming

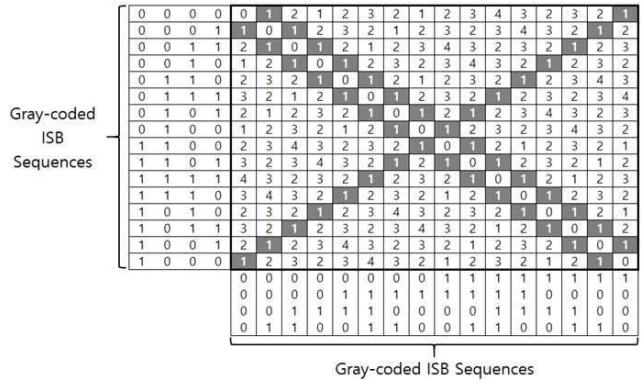

FIGURE 2. The 2D Hamming distance table of the Gray-coded ISB sequences when $p_1 = 4$.

distances (i.e., 1's) of the Gray-coded ISB sequences. The i-th binary sequences of length n for $i = 1, 2, \cdots, 2^n$ is defined as

$$\mathbf{V}_i = [\, v_{i,n}\ v_{i,n-1}\ \cdots\ v_{i,1}\,], \tag{25}$$

where $v_{i,l} \in \{0, 1\}$, $l = 1, 2, \cdots, n$. Note that $v_{i,n}$ and $v_{i,1}$ correspond to the MSB and the LSB of $\mathbf{V}_i$, respectively. The SAP candidate sequences are generated by selecting the N_{SAP} sequences with k 1's and $(n-k)$ 0's from $\{\mathbf{V}_i\}_{i=1}^{2^n}$ in consecutive order. The i-th SAP candidate sequence for $i = 1, 2, \cdots, N_{\mathrm{SAP}}$ is defined as

$$\mathbf{G}_i = [\, g_{i,n}\ g_{i,n-1}\ \cdots\ g_{i,1}\,]. \tag{26}$$

Since every sequence in $\{\mathbf{G}_i\}_{i=1}^{N_{\mathrm{SAP}}}$ consists of k 1's and $(n-k)$ 0's, the minimum Hamming distance of $\{\mathbf{G}_i\}_{i=1}^{N_{\mathrm{SAP}}}$ is given by 2. The proposed index mapping algorithm selects 2^{p_1} SAP candidate sequences from $\{\mathbf{G}_i\}_{i=1}^{N_{\mathrm{SAP}}}$ in a desired order. The indices of the selected SAP candidate sequences can be written in a vector form as

$$\mathcal{I}_{\mathrm{SAP}} = [\, i_1, i_2, \cdots, i_{2^{p_1}}\,], \tag{27}$$

where $1 \le i_1 < i_2 < \cdots < i_{2^{p_1}} \le N_{\mathrm{SAP}}$. If a suitable $\mathcal{I}_{\mathrm{SAP}}$ is found, the SAP sequences that are mapped to $\{\mathbf{ISB}_\eta\}_{\eta=1}^{2^{p_1}}$ in consecutive order are determined by

$$\mathbf{SAP}_\eta = \mathbf{G}_{i_\eta} \tag{28}$$

for $\eta = 1, 2, \cdots, 2^{p_1}$. The purpose of the proposed index mapping algorithm is to find a suitable $\mathcal{I}_{\mathrm{SAP}}$, which can make the minimum Hamming distances (i.e., 2's) of $\{\mathbf{G}_{i_\eta}\}_{\eta=1}^{2^{p_1}}$ be located in the same X-shaped cross as that of the minimum Hamming distances of $\{\mathbf{ISB}_\eta\}_{\eta=1}^{2^{p_1}}$ on the 2D Hamming distance table. In the proposed index mapping algorithm, a suitable $\mathcal{I}_{\mathrm{SAP}}$ is searched on an iteration basis by inducing $\mathbf{G}_{i_\eta}$ to have minimum Hamming distance 2 not only with $\mathbf{G}_{i_{\eta+1}}$ but also with $\mathbf{G}_{i_{2^{p_1}-\eta+1}}$ for $\eta = 1, 2, \cdots, 2^{p_1} - 1$. The proposed index mapping algorithm is reified as a pseudo-code in Algorithm 1. The parameters and the variables used in Algorithm 1 are as follows:

- $d_{\min}$: the target minimum Hamming distance of the SAP sequences, which is set as 2.

Algorithm 1 Pseudo-Code for the Proposed Index Mapping Algorithm

$d_{\min} = 2$
$p_1 = \lfloor \log_2(N_{\mathrm{SAP}}) \rfloor$
$\mathcal{P} = \{1, 2, \cdots, N_{\mathrm{SAP}}\}$
$\mathcal{I}_{\mathrm{F}} = [\,],\ \mathcal{I}_{\mathrm{L}} = [\,]$
while $len(\mathcal{I}_F) + len(\mathcal{I}_F) < 2^{p_1}$ *and* $len(\mathcal{P}) > 0$ **do**
  $\mathcal{P}_{\mathrm{asce}} = \mathrm{sort}(\mathcal{P}, \text{'ascending'})$
  for $i_{F,new} \in \mathcal{P}_{asce}$ **do**
    if $len(\mathcal{I}_F) = 0$ *or* $dist(\mathbf{G}_{i_{F,new}}, \mathbf{G}_{i_{F,old}}) = d_{min}$ **then**
      break
    end
  end
  $\mathcal{P}_{\mathrm{desc}} = \mathrm{sort}(\mathcal{P}, \text{'descending'})$
  $\mathrm{flag} = 0$
  for $i_{L,new} \in \mathcal{P}_{desc}$ **do**
    if $dist(\mathbf{G}_{i_{L,new}}, \mathbf{G}_{i_{F,new}}) = d_{min}$ **then**
      if $len(\mathcal{I}_L) = 0$ *or* $dist(\mathbf{G}_{i_{L,new}}, \mathbf{G}_{i_{L,old}}) = d_{min}$ **then**
        $\mathrm{flag} = 1$
        break
      end
    end
  end
  if $flag = 1$ **then**
    $\mathcal{I}_{\mathrm{F}} = [\, \mathcal{I}_{\mathrm{F}}(1), \mathcal{I}_{\mathrm{F}}(2), \cdots, \mathcal{I}_{\mathrm{F}}(\mathrm{len}(\mathcal{I}_{\mathrm{F}})), i_{\mathrm{F,new}}\,]$
    $\mathcal{I}_{\mathrm{L}} = [\, i_{\mathrm{L,new}}, \mathcal{I}_{\mathrm{L}}(1), \mathcal{I}_{\mathrm{L}}(2), \cdots, \mathcal{I}_{\mathrm{L}}(\mathrm{len}(\mathcal{I}_{\mathrm{L}}))\,]$
    $i_{\mathrm{F,old}} = i_{\mathrm{F,new}}$
    $i_{\mathrm{L,old}} = i_{\mathrm{L,new}}$
    $\mathcal{P} = \mathcal{P} - \{i_{\mathrm{F,new}}, i_{\mathrm{L,new}}\}$
  end
  else
    $\mathcal{P} = \mathcal{P} - \{i_{\mathrm{F,new}}\}$
  end
end
$\mathcal{I}_{\mathrm{SAP}} = [\, \mathcal{I}_{\mathrm{F}}(1), \cdots, \mathcal{I}_{\mathrm{F}}(\mathrm{len}(\mathcal{I}_{\mathrm{F}})), \mathcal{I}_{\mathrm{L}}(1), \cdots, \mathcal{I}_{\mathrm{L}}(\mathrm{len}(\mathcal{I}_{\mathrm{L}}))\,]$
if $len(\mathcal{I}_{SAP}) \neq 2^{p_1}$ **then**
  $p_1 = \lfloor \log_2 \left(\mathrm{len}(\mathcal{I}_{\mathrm{SAP}})\right) \rfloor$
end

- $\{\mathbf{G}_i\}_{i=1}^{N_{\mathrm{SAP}}}$: the SAP candidates sequences, from which the SAP sequences, $\{\mathbf{SAP}_\eta\}_{\eta=1}^{2^{p_1}}$, are selected.
- $\mathcal{I}_{\mathrm{F}}$: the index vector representing the former part of $\mathcal{I}_{\mathrm{SAP}}$. It is initialized as $\mathcal{I}_{\mathrm{F}} = [\,]$.
- $\mathcal{I}_{\mathrm{L}}$: the index vector representing the latter part of $\mathcal{I}_{\mathrm{SAP}}$. It is initialized as $\mathcal{I}_{\mathrm{L}} = [\,]$.
- $\mathcal{P}$: the index pool set, whose components correspond to the index candidates for selecting a new SAP sequence from $\{\mathbf{G}_i\}_{i=1}^{N_{\mathrm{SAP}}}$. It is initialized as $\mathcal{P} = \{1, 2, \cdots, N_{\mathrm{SAP}}\}$.
- $\mathcal{P}_{\mathrm{asce}}$: the index pool set sorted in ascending order.
- $\mathcal{P}_{\mathrm{desc}}$: the index pool set sorted in descending order.
- $i_{\mathrm{F,new}}$: the foremost component of $\mathcal{P}_{\mathrm{asce}}$ satisfying (30).
- $i_{\mathrm{F,old}}$: the value of $i_{\mathrm{F,new}}$ chosen previously.

- $i_{\mathrm{L,new}}$: the foremost component of $\mathcal{P}_{\mathrm{desc}}$ satisfying (32) and (33).
- $i_{\mathrm{L,old}}$: the value of $i_{\mathrm{L,new}}$ chosen previously.

In Algorithm 1, an algorithmic loop is repeated as long as $\mathrm{len}(\mathcal{I}_F)+\mathrm{len}(\mathcal{I}_L) < 2^{p_1}$ and $\mathrm{len}(\mathcal{P}) > 0$. If $\mathcal{P} = [\ ]$, the algorithmic loop terminates because a new index cannot be chosen from $\mathcal{P}$. $\mathcal{P}_{\mathrm{asce}}$ is prepared by sorting the components of $\mathcal{P}$ in ascending order, which is expressed as

$$\mathcal{P}_{\mathrm{asce}} = \mathrm{sort}\,(\mathcal{P}, \text{'ascending'})\,. \tag{29}$$

In the first step of the algorithmic loop, if $\mathrm{len}(\mathcal{I}_{\mathrm{F}}) = 0$, $i_{\mathrm{F,new}}$ is chosen as 1 (i.e., the foremost component of $\mathcal{P}_{\mathrm{asce}}$ at the beginning) and if $\mathrm{len}(\mathcal{I}_{\mathrm{F}}) > 0$, $i_{\mathrm{F,new}}$ is chosen as the foremost component of $\mathcal{P}_{\mathrm{asce}}$ satisfying

$$\mathrm{dist}(\mathbf{G}_{i_{\mathrm{F,new}}}, \mathbf{G}_{i_{\mathrm{F,old}}}) = d_{\min}. \tag{30}$$

The constraint of (30) is necessary to induce $\mathbf{SAP}_{\eta}$ to have minimum Hamming distance 2 with $\mathbf{SAP}_{\eta+1}$ for $\eta = 1, 2, \cdots, 2^{p_1} - 1$. If any component is chosen from $\mathcal{P}_{\mathrm{asce}}$ for $i_{\mathrm{F,new}}$, then $\mathcal{P}_{\mathrm{desc}}$ is prepared by sorting the components of $\mathcal{P}$ in descending order as

$$\mathcal{P}_{\mathrm{desc}} = \mathrm{sort}\,(\mathcal{P}, \text{'descending'})\,. \tag{31}$$

In the second step of the algorithmic loop, if $\mathrm{len}(\mathcal{I}_{\mathrm{L}}) = 0$, $i_{\mathrm{L,new}}$ is chosen as N_{SAP} (i.e., the foremost component of $\mathcal{P}_{\mathrm{desc}}$ at the beginning) and if $\mathrm{len}(\mathcal{I}_{\mathrm{L}}) > 0$, $i_{\mathrm{L,new}}$ is chosen as the foremost component of $\mathcal{P}_{\mathrm{desc}}$ satisfying

$$\mathrm{dist}(\mathbf{G}_{i_{\mathrm{L,new}}}, \mathbf{G}_{i_{\mathrm{F,new}}}) = 2, \tag{32}$$
$$\mathrm{dist}(\mathbf{G}_{i_{\mathrm{L,new}}}, \mathbf{G}_{i_{\mathrm{L,old}}}) = 2. \tag{33}$$

The constraint of (32) is necessary to induce $\mathbf{SAP}_{\eta}$ to have minimum Hamming distance 2 with $\mathbf{SAP}_{2^{p_1}-\eta+1}$ for $\eta = 1, 2, \cdots, 2^{p_1-1}$, whereas the constraint of (33) is necessary to induce $\mathbf{SAP}_{\eta}$ to have minimum Hamming distance 2 with $\mathbf{SAP}_{\eta+1}$ for $\eta = 1, 2, \cdots, 2^{p_1} - 1$. If no component is found from $\mathcal{P}_{\mathrm{desc}}$ for $i_{\mathrm{L,new}}$, the value of $i_{\mathrm{F,new}}$ is removed from $\mathcal{P}$ as

$$\mathcal{P} = \mathcal{P} - \{\, i_{\mathrm{F,new}} \,\} \tag{34}$$

and the algorithmic loop restarts at the first step. If any component is chosen from $\mathcal{P}_{\mathrm{desc}}$ for $i_{\mathrm{L,new}}$, the values of $i_{\mathrm{F,new}}$ and $i_{\mathrm{L,new}}$ are added to $\mathcal{I}_{\mathrm{F}}$ and $\mathcal{I}_{\mathrm{L}}$, respectively, as

$$\mathcal{I}_{\mathrm{F}} = [\,\mathcal{I}_{\mathrm{F}}(1),\ \cdots,\ \mathcal{I}_{\mathrm{F}}(\mathrm{len}(\mathcal{I}_{\mathrm{F}})),\ i_{\mathrm{F,new}}\,], \tag{35}$$
$$\mathcal{I}_{\mathrm{L}} = [\,i_{\mathrm{L,new}},\ \mathcal{I}_{\mathrm{L}}(1),\ \cdots,\ \mathcal{I}_{\mathrm{L}}(\mathrm{len}(\mathcal{I}_{\mathrm{L}}))\,]. \tag{36}$$

Then, the values of $i_{\mathrm{F,old}}$ and $i_{\mathrm{L,old}}$ are updated as

$$i_{\mathrm{F,old}} = i_{\mathrm{F,new}}, \tag{37}$$
$$i_{\mathrm{L,old}} = i_{\mathrm{L,new}}, \tag{38}$$

and $\mathcal{P}$ is updated as

$$\mathcal{P} = \mathcal{P} - \{i_{\mathrm{F,new}},\ i_{\mathrm{L,new}}\}. \tag{39}$$

In this manner, the algorithmic loop repeats as long as the condition of $\mathrm{len}(\mathcal{I}_{\mathrm{F}}) + \mathrm{len}(\mathcal{I}_{\mathrm{F}}) < 2^{p_1}$ or that of $\mathrm{len}(\mathcal{P}) > 0$ holds. Once the search of $\mathcal{I}_{\mathrm{F}}$ and $\mathcal{I}_{\mathrm{L}}$ finishes under the constraint of $\mathrm{len}\{\mathcal{I}_F\}+\mathrm{len}\{\mathcal{I}_L\} = 2^{p_1}$, $\mathcal{I}_{\mathrm{SAP}}$ is finally determined as

$$\mathcal{I}_{\mathrm{SAP}} = [\,\mathcal{I}_{\mathrm{F}}(1),\ \cdots,\ \mathcal{I}_{\mathrm{F}}(\mathrm{len}(\mathcal{I}_{\mathrm{F}})),\ \mathcal{I}_{\mathrm{L}}(1),\ \cdots,\ \mathcal{I}_{\mathrm{L}}(\mathrm{len}(\mathcal{I}_{\mathrm{L}}))\,]. \tag{40}$$

If the algorithmic loop terminates under the constraint of $\mathrm{len}(\mathcal{P}) = 0$, the number of the components in $\mathcal{I}_{\mathrm{SAP}}$ may be different from 2^{p_1}, which implies that the proposed index mapping strategy does not hold with the given value of p_1. In such a case, the value of p_1 should be changed as $p_1 = \lfloor \log_2 \left(\mathrm{len}(\mathcal{I}_{\mathrm{SAP}})\right) \rfloor$ to fulfill our mapping strategy. In Fig. 3, the mapping results by the proposed index mapping algorithm are provided for three cases of (a) $(n, k, p_1) = (4, 2, 2)$ (b) $(n, k, p_1) = (6, 3, 4)$, and (c) $(n, k, p_1) = (8, 3, 5)$. In Fig. 4 (a), the 2D Hamming distance table of the searched SAP sequences for the case of $(n, k, p_1) = (6, 3, 4)$ is presented. It can be seen that the minimum Hamming distances (i.e., 2's) of the 16 SAP sequences are located in the same X-shaped cross as that of the minimum Hamming distances (i.e., 1's) of the 16 Gray-coded ISB sequences as shown in Fig. 2. The minimum Hamming distances of the SAP sequences that were found by the proposed index mapping algorithm for the case of $(n, k, p_1) = (4, 2, 2)$ or $(n, k, p_1) = (8, 3, 5)$ are also located in the same X-shaped cross as that of the minimum Hamming distances of the corresponding Gray-coded ISB sequences.

(a)

ISB	SAP
0 0	0 1 0 1
0 1	0 1 1 0
1 1	1 0 1 0
1 0	1 0 0 1

(b)

ISB	SAP
0 0 0	0 0 0 1 1 1
0 0 1	0 0 1 0 1 1
0 1 1	0 0 1 1 0 1
0 1 0	0 0 1 1 1 0
0 1 1	0 1 0 1 1 0
0 1 1	0 1 0 0 1 1
0 1 0	0 1 0 1 0 1
1 1 0	0 1 1 1 0 0
1 1 1	0 1 1 0 0 1
1 1 1	0 1 1 0 1 0
1 1 0	0 1 1 1 1 0
1 0 1	0 1 1 1 0 0
1 0 1	0 1 1 1 0 0
1 0 0	0 1 1 1 1 1

(c)

ISB	SAP
0 0 0 0 0	0 0 0 0 0 1 1 1
0 0 0 0 1	0 0 0 0 0 1 0 1 1
0 0 0 1 1	0 0 0 0 0 1 1 0 1
0 0 0 1 0	0 0 0 0 0 1 1 1 0
0 0 1 1 0	0 0 0 0 1 0 1 1 0
0 0 1 1 1	0 0 0 0 1 0 0 1 1
0 0 1 0 1	0 0 0 0 1 0 1 0 1
0 0 1 0 0	0 0 0 0 1 1 0 0 1
0 1 1 0 0	0 0 0 0 1 1 0 1 0
0 1 1 0 1	0 0 0 0 1 1 1 0 0
0 1 1 1 1	0 0 1 0 1 1 0 0
0 1 1 1 0	0 0 1 0 0 0 1 0 1
0 1 0 1 0	0 0 1 0 0 0 1 1 1
0 1 0 1 1	0 0 1 0 0 1 1 0
0 1 0 0 1	0 0 1 0 1 0 1 0
0 1 0 0 0	0 0 1 0 1 1 0 0 1
1 1 0 0 0	1 0 1 0 1 0 0 0
1 1 0 0 1	0 1 1 0 1 0 0 0
1 1 0 1 1	0 1 1 0 0 0 1 0
1 1 0 1 0	1 0 1 0 0 0 1 0
1 1 1 1 0	1 0 1 0 0 0 0 1
1 1 1 1 1	1 0 1 0 0 1 0 0
1 1 1 0 1	1 0 0 1 0 1 0 0
1 1 1 0 0	1 0 0 1 1 0 0 0
1 0 1 0 0	1 0 0 1 0 0 0 1
1 0 1 0 1	0 1 0 1 0 0 0 1
1 0 1 1 1	0 1 0 1 0 0 1 0
1 0 1 1 0	0 1 0 1 0 1 0 0
1 0 0 1 0	0 1 0 0 1 1 0 0
1 0 0 1 1	1 0 0 0 1 1 0 0
1 0 0 0 1	1 0 0 0 1 0 1 0
1 0 0 0 0	1 0 0 0 0 1 1 0

FIGURE 3. The proposed index mapping between the SAP and ISB sequences in three cases of (a) $(n, k, p_1) = (4, 2, 2)$, (b) $(n, k, p_1) = (6, 3, 4)$, and (c) $(n, k, p_1) = (8, 3, 5)$.

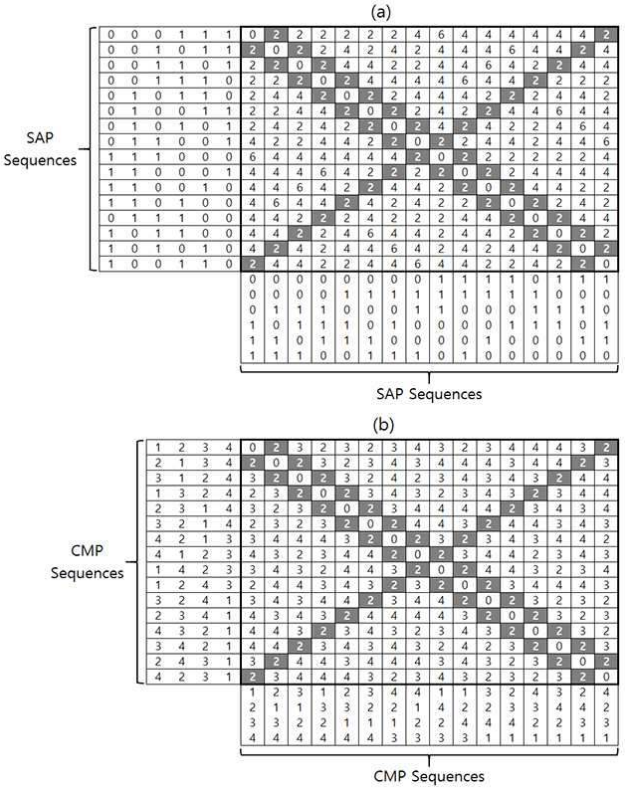

FIGURE 4. The 2D Hamming distance tables of (a) the SAP sequences in the case of $(n, k, p_1)=(6, 3, 4)$ and (b) the CMP sequences in the case of $(n, p_1)=(4, 4)$.

B. INDEX MAPPING FOR CI-MM-OFDM-IM

The proposed index mapping algorithm can also be applied to CI-MM-OFDM-IM to find a mapping between the ISB and CMP sequences. In order to apply Algorithm 1 for CI-MM-OFDM-IM, it is necessary to change the following:

1. $\mathcal{I}_{\text{SAP}}$ in Algorithm 1 should be replaced with $\mathcal{I}_{\text{CMP}}$.
2. N_{SAP} in Algorithm 1 should be replaced with N_{CMP} whose value is given by $n!$.
3. $\{\mathbf{G}_i\}_{i=1}^{N_{\text{CMP}}}$ in Algorithm 1 should be determined by $n!$ permutations of $\{1, 2, \cdots, n\}$ in consecutive order, where $\mathbf{G}_1$ and $\mathbf{G}_{n!}$ are given by $[1, 2, \cdots, n]$ and $[n, n-1, \cdots, 1]$, respectively.

Once a suitable $\mathcal{I}_{\text{CMP}}$ is found by Algorithm 1, the CMP sequences that are mapped to the Gray-coded ISB sequences, $\{\mathbf{ISB}\}_{\eta=1}^{2^{p_1}}$, in consecutive order are determined by

$$\mathbf{CMP}_\eta = \mathbf{G}_{i_\eta} \tag{41}$$

for $\eta = 1, 2, \cdots, 2^{p_1}$, where i_η denotes the η-th component of $\mathcal{I}_{\text{CMP}}$. In Fig. 4 (b), the 2D Hamming distance table of the CMP sequences is presented for the case of $(n, p_1) = (4, 4)$. By comparing Fig. 4 (b) with Fig. 2, it can be seen that the minimum Hamming distances (i.e., 2's) of the 16 CMP sequences are located in the same X-shaped cross as that of the minimum Hamming distances (i.e., 1's) of the 16 Gray-coded ISB sequences.

IV. DISCUSSION

• If exhaustive search were used instead of Algorithm 1 in finding an optimal mapping, the 'dist' function would be executed $N_{\text{SAP}}! \times N_{\text{SAP}}(N_{\text{SAP}} - 1)$ or $N_{\text{CMP}}! \times (N_{\text{CMP}} - 1)$ times. However, it is too large a number for practical use even with small-sized n. For example, given $(n, k, p_1) = (8, 3, 5)$ for OFDM-IQ-IM, exhaustive search needs to execute the 'dist' function 2.19×10^{78} times, whereas Algorithm 1 needs to execute the 'dist' and 'sort' functions only 58 and 32 times, respectively.

• In Algorithm 1, $d_{\min}$ of the SAP (or CMP) sequences can be chosen larger than 2 to further enhance the BER performance. If the SAP (or CMP) candidate sequences $\{\mathbf{G}_i\}_{i=1}^{N_{\text{SAP}}}$ with minimum Hamming distance larger than 2 are inputted into Algorithm 1 and $d_{\min}$ is set to the same value as the minimum Hamming distance of $\{\mathbf{G}_i\}_{i=1}^{N_{\text{SAP}}}$, Algorithm 1 can generate the SAP (or CMP) sequences that enhance the BER performance further because of the increased minimum Hamming distance as well as the effect of the proposed index mapping strategy. However, by choosing $d_{\min}$ larger than 2 the number of the searched SAP (or CMP) sequences decreases due to the limited degree of freedom in generating those sequences. In other words, choosing $d_{\min}$ larger than 2 may result in the reduced spectral efficiency of an OFDM-IM system. Since the primary purpose of our paper is to improve the BER performance of an OFDM-IM system without losing spectral efficiency for a given subblock size, we focus on the search of the SAP (or CMP) sequences under the assumption of minimum Hamming distance 2.

• The conventional index mapping according to the combinatorial method does not require a mapping table because the combinatorial method computes the index of an SAP sequence directly by using an ISB sequence. However, the combinatorial method may incur an unexpected catastrophic failure in retrieving the SAP sequence ([6]). Therefore, the proposed index mapping that uses a mapping table can outperform the conventional index mapping.

• In the proposed index mapping, since the SAP (or CMP) sequences are determined by a mapping strategy of locating the minimum Hamming distances (i.e., 2's) of the SAP (or CMP) sequences in the same X-shaped cross as that of the minimum Hamming distances (i.e., 1's) of the Gray-coded ISB sequences, not every pair of the SAP (or CMP) sequences which have minimum distance 2 is associated with a separate pair of ISB sequences which have minimum distance 1. For example, in the case of $(n, k, p_1) = (6, 3, 4)$, the 2D Hamming distance table of the SAP sequences as shown in Fig. 4 (a) contains 114 2's, where only 48 2's (i.e. 42.1% of 2's) in the table are mapped to the 48 1's in the 2D Hamming distance table of the ISB sequences as shown in Fig. 2. As n increases, the proposed index mapping can associate a less portion of the pairs of SAP (or CMP) sequences which have minimum distance 2 with a separate pair of ISB sequences which have minimum distance 1. For example, in the case of $(n, k, p_1) = (8, 3, 5)$, the 2D Hamming distance table of the SAP sequences contains 298 2's, where only 106

2's (i.e. 35.6% of 2's) in the table are mapped to the 106 1's in the 2D Hamming distance table of the ISB sequences. Therefore, the gain of the proposed index mapping over the conventional index mapping decreases as the subblock size, n, increases.

• The BER performance of OFDM-IQ-IM can be further improved by generating SAP (or CMP) sequences by concatenating multiple short SAP (or CMP) sequences designed for smaller-sized subblocks because short SAP (or CMP) sequences are less affected by error propagation. However, generating SAP (or CMP) sequences by concatenating multiple short SAP (or CMP) sequences may reduce the number of the index bits due to the limited degree of freedom in generating the SAP (or CMP) sequences. In [25], it was shown that in the three cases of $(n, k) = (4, 2)$, $(n, k) = (8, 2)$, and $(n, k) = (8, 6)$, the approach of generating SAP (or CMP) sequences by concatenating two short SAP (or CMP) sequences does not reduce the number of index bits. For example, in the case of a dual-mode IM with $(n, k) = (4, 2)$, the number of index bits is given by $p_1 = \lfloor \log_2({}_4C_2) \rfloor = 2$, whereas the number of index bits for the CMP sequences generated by concatenating 2 short CMP sequences designed for the case of a dual-mode IM with $(n, k) = (2, 1)$ is given by $\lfloor \log_2({}_2C_1 \times {}_2C_1) \rfloor = 2$. Therefore, in the case of a dual-mode IM with $(n, k) = (4, 2)$, total 4 CMP sequences of length 4 can be generated by concatenating 2 CMP sequences of length 2 designed for the case of a dual-mode IM with $(n, k) = (2, 1)$ for a better BER performance but without losing SE. The resultant CMP sequences are given as $[M_A\, M_B\, M_A\, M_B]$, $[M_A\, M_B\, M_B\, M_A]$, $[M_B\, M_A\, M_A\, M_B]$, and $[M_B\, M_A\, M_B\, M_A]$, where M_A and M_B denote two symbol constellation modes. If these sequences are used as the CMP candidate sequences, $\{\mathbf{G}_i\}_{i=1}^{N_{\mathrm{CMP}}}$, in Algorithm 1 with the initial values of $N_{\mathrm{CMP}} = 4$ and $p_1 = 2$, Algorithm 1 can generate the CMP sequences that comply with the proposed index mapping strategy as $\mathbf{CMP}_1 = [M_A\, M_B\, M_A\, M_B]$, $\mathbf{CMP}_2 = [M_A\, M_B\, M_B\, M_A]$, $\mathbf{CMP}_3 = [M_B\, M_A\, M_B\, M_A]$, and $\mathbf{CMP}_4 = [M_B\, M_A\, M_A\, M_B]$. Note that these CMP sequences are consecutively mapped to the Gray-coded ISB sequences, $\mathbf{ISB}_1 = [0\,0]$, $\mathbf{ISB}_2 = [0\,1]$, $\mathbf{ISB}_3 = [1\,1]$, and $\mathbf{ISB}_4 = [1\,0]$. This mapping results are the same as those suggested in [23].

V. SIMULATION RESULTS

With the conventional index mapping in OFDM-IQ-IM, the ISB sequences, $\{\mathbf{ISB}_\eta\}_{\eta=1}^{2^{p_1}}$, are generated by

$$\mathbf{ISB}_\eta = \mathbf{B}_\eta \tag{42}$$

for $\eta = 1, 2, \cdots, 2^{p_1}$ and the SAP sequences, $\{\mathbf{SAP}_\eta\}_{\eta=1}^{2^{p_1}}$, are generated by selecting the first 2^{p_1} sequences consisting of k 1's and $(n - k)$ 0's from $\{\mathbf{V}_\eta\}_{\eta=1}^{2^n}$. Note that the conventional index mapping that associates $\{\mathbf{SAP}_\eta\}_{\eta=1}^{2^{p_1}}$ with $\{\mathbf{ISB}_\eta\}_{\eta=1}^{2^{p_1}}$ in consecutive order is equivalent to the index mapping based on the combinatorial method in [6]. With the conventional index mapping in CI-MM-OFDM-IM, the ISB sequences, $\{\mathbf{ISB}_\eta\}_{\eta=1}^{2^{p_1}}$, are generated by (42) and the CMP sequences, $\{\mathbf{CMP}_\eta\}_{\eta=1}^{2^{p_1}}$, are generated by selecting the first 2^{p_1} sequences from the $n!$ permutations of $\{1, 2, \cdots, n\}$. The simulation parameters commonly used in this section are summarized in Table 1.

TABLE 1. The simulation parameters commonly used in Section V.

Parameter	Value
OFDM block size N	128
Cyclic prefix length L_c	16
Effective channel length ν	10
Convolutional code rate R	1/3, 1/2, or 2/3

Generation polynomial for R=1/3 is (133,171,165) in octal ([26]), that for R=1/2 is (171,133) in octal ([27]), and that for R=2/3 is (23,35,0;0,5,13) in octal ([28]).

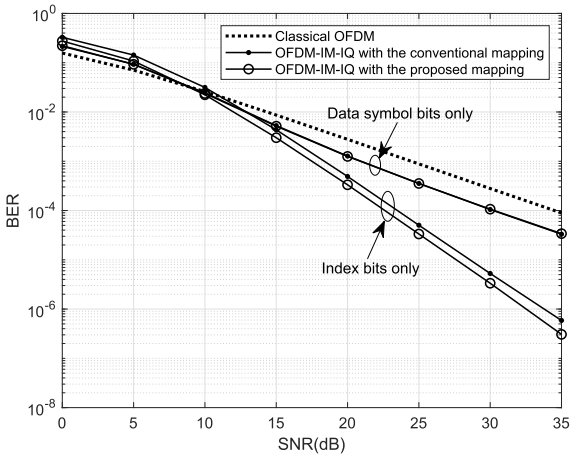

FIGURE 5. Comparison of the BER results of classical OFDM and two OFDM-IQ-IM schemes in the case of $(n, k, p_1) = (8, 3, 5)$, where the BERs of the index and data symbol bits are evaluated separately.

In Fig. 5, the BER performances of classical OFDM, OFDM-IQ-IM with the proposed index mapping, and OFDM-IQ-IM with the conventional index mapping are compared in the case of $(n, k, p_1) = (8, 3, 5)$ when 4QAM is used for classical OFDM and binary PAM is used for the I- and Q- branches of OFDM-IQ-IM. The spectral efficiencies of all the three schemes are given by 1.78 bits/s/Hz. Herein, the BERs of the index and data symbol bits are evaluated separately. From the figure, we observe that at a high SNR, the BER performance of the index bits is much better than that of the data symbol bits in both the OFDM-IQ-IM schemes. This observation is consistent with the derivation result of the pairwise error probability for an OFDM-IM system in [6], which showed that at a high SNR the diversity order of the index bits is greater than or equal to 2, whereas that of the data symbol bits is 1. In addition, we observe that the proposed index mapping improves the BER performance of the index bits compared to that of the conventional index mapping; the proposed index mapping attains 0.9dB SNR gain over the conventional index mapping at the BER of 10^{-4}.

In Fig. 6, the BER performances of classical OFDM, OFDM-IQ-IM with the proposed index mapping, and

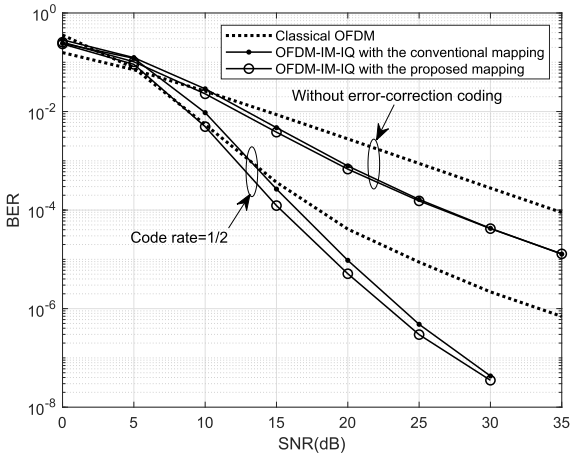

FIGURE 6. Comparison of the BER results of classical OFDM and two OFDM-IQ-IM schemes in the case of $(n, k, p_1) = (8, 3, 5)$.

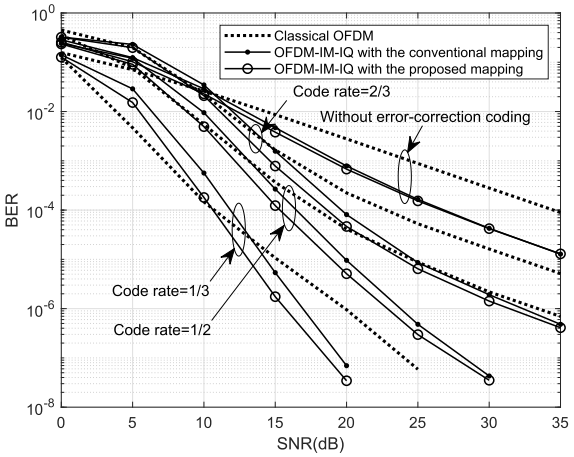

FIGURE 7. Comparison of the BER results of classical OFDM and two OFDM-IQ-IM schemes in the case of $(n, k, p_1) = (8, 3, 5)$ when different error-correction code rates are applied.

OFDM-IQ-IM with the conventional index mapping are compared under the same parameters as given for Fig. 5, but herein, the BERs are found by evaluating the index and data symbol bits together. From the BER curves without using an error correction code, we observe that whereas the gain of the proposed index mapping over the conventional index mapping tends to increase as the SNR decreases, the proposed index mapping attains only a trivial SNR gain over the conventional index mapping at the BER of 10^{-4}. It is because the gain of the proposed index mapping over the conventional index mapping obtained with the index bits is concealed by the comparably worse performance of the data symbol bits. Note that if the BER of the data symbol bits becomes comparable to that of the index bits by help of error correction coding, the proposed index mapping can improve the BER performance more conspicuously even when the index and data symbol bits are evaluated simultaneously. In order to investigate the impact of an error correction code on the performance of IM, the BERs of the three schemes are evaluated by applying a rate-half convolutional code ([26]) and a random interleaver which rearranges the elements of the coded bits using a random permutation ([29]). Provided with a rate-half convolutional code, the spectral efficiencies of all the three schemes are given by 0.89 bits/s/Hz. From the BER curves obtained by applying a rate-half convolutional code, we observe that the proposed index mapping attains 1dB SNR gain over the conventional index mapping at the BER of 10^{-4}. It corroborates our argument that the proposed index mapping can extract more gain over the conventional index mapping by applying an error-correction code.

In Fig. 7, the BER performances are evaluated under the same parameters as given for Fig. 6, but herein, by applying three convolutional codes with code rates of $R = \frac{1}{3}$, $R = \frac{1}{2}$, and $R = \frac{2}{3}$. From the figure, we observe that the gain of the proposed index mapping over the conventional index mapping increases as the code rate decreases at the BER of 10^{-4}; with the error-correction code of code rate $R = \frac{1}{3}$, the gain of the proposed index mapping over the conventional index mapping reaches 1.2dB at the BER of 10^{-4}. It certifies that since using an intense error-correction code helps the BER of data symbol bits be further comparable to that of the index bits, it can enhance performance of an efficient index mapping.

In Fig. 8, the impact of the symbol constellation size on the performance gain of the proposed index mapping was investigated by comparing the BER performances in two cases. In the first case, 4QAM is used for classical OFDM and binary PAM is used for the I- and Q- branches of OFDM-IQ-IM as in Fig. 6. In the second case, 16QAM is used for classical OFDM and 4-ary PAM is used for the I- and Q- branches of OFDM-IQ-IM. From the figure, we observe that the gain of the proposed index mapping over the conventional index mapping reduces as the adopted symbol constellation size increases; while the proposed index mapping obtained 1dB SNR gain over the conventional index at the BER of 10^{-4} in the first case, the proposed index mapping obtained only 0.8dB SNR gain in the second case. The gain of the proposed index mapping over the conventional index mapping diminishes with a larger symbol constellation size because the BER improvement of the index bits given by the proposed index mapping is blurred out by the worse BER of the data symbols selected from a larger symbol constellation.

In Fig. 9, the BER performances of classical OFDM, CI-MM-OFDM-IM with the proposed index mapping, and CI-MM-OFDM-IM with the conventional index mapping are compared in the case of $(n, p_1) = (4, 4)$ when 4QAM is used for classical OFDM and 8-ary PSK is used for CI-MM-OFDM-IM. The value of θ is set as $\theta = 8.6°$ as given in [10]. In order to investigate the impact of an error correction code on the performance of IM, the BERs of the three schemes are found by applying three convolutional codes with code rates of $R = \frac{1}{3}$, $R = \frac{1}{2}$, and $R = \frac{2}{3}$ and a random interleaver ([29]). Without an error correction code, the proposed index

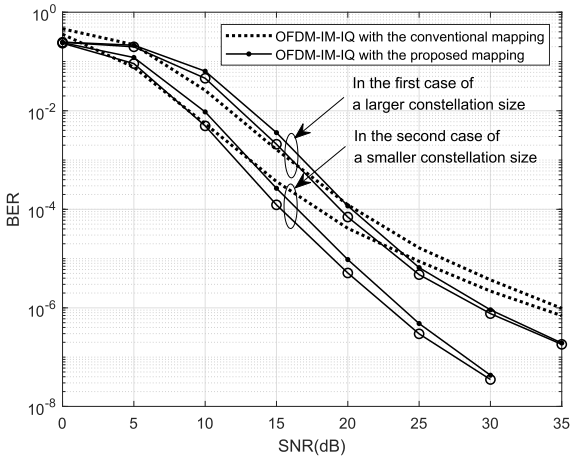

FIGURE 8. Comparison of the BER results of classical OFDM and two OFDM-IQ-IM schemes in the case of $(n, k, p_1)=(8, 3, 5)$ when different symbol constellation sizes are adopted.

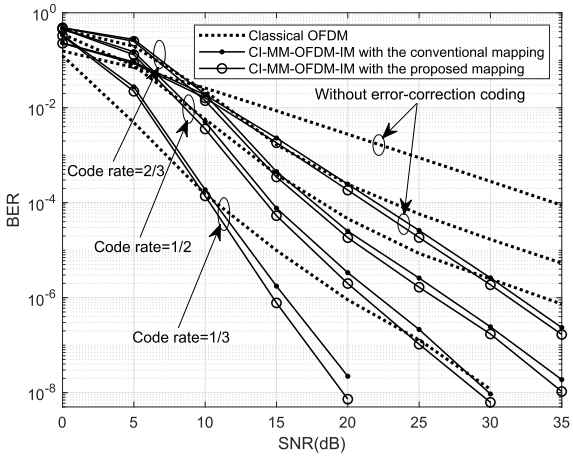

FIGURE 9. Comparison of the BER results of classical OFDM and two CI-MM-OFDM-IM schemes in the case of $(n, p_1)=(4, 4)$.

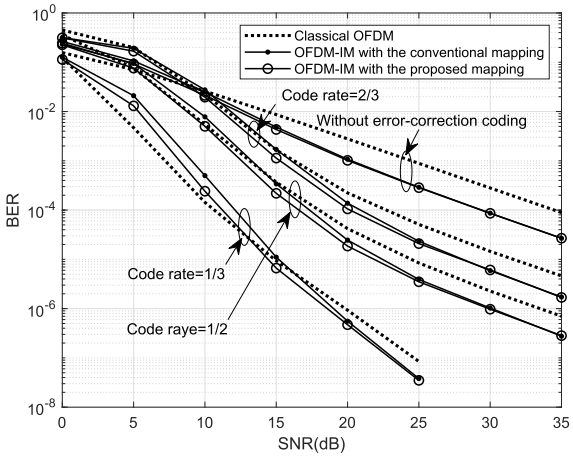

FIGURE 10. Comparison of the BER results of classical OFDM and two OFDM-IM schemes in the case of $(n, k, p_1)=(8, 3, 5)$ when 4QAM is used for all the three schemes.

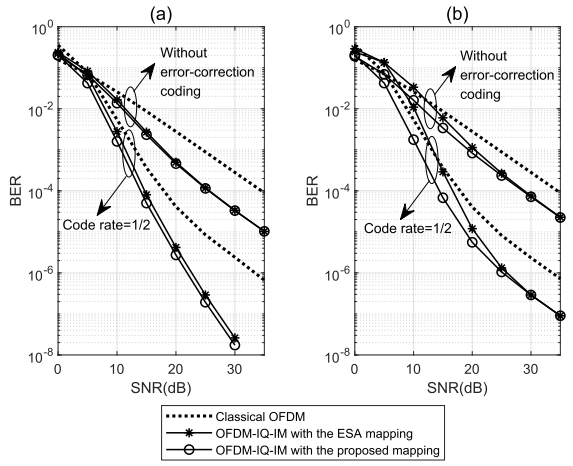

FIGURE 11. Comparison of the BER results of classical OFDM, OFDM-IQ-IM with the proposed index mapping, and OFDM-IQ-IM with the ESA mapping ([22]) in two cases of (a) $(n, k, p_1)=(8, 2, 4)$ and (b) $(n, k, p_1)=(8, 4, 5)$.

mapping attained 0.59dB SNR gain over the conventional index mapping at the BER of 10^{-6}. By applying an error correction code, the proposed index mapping extracted a larger gain over the conventional index mapping. Similarly to the case of OFDM-IQ-IM in Fig. 7, we observe from Fig. 9 that the gain of the proposed index mapping in the case of CC-MM-OFDM-IM increases as the code rate decreases.

In Fig. 10, the BER performances of classical OFDM, OFDM-IM ([6]) with the proposed index mapping, and OFDM-IM with the conventional index mapping are compared in the case of $(n, k, p_1)=(8, 3, 5)$ when 4QAM is used for all the three schemes. In order to investigate the impact of an error correction code on the performance of IM, the BERs of the three schemes are found by applying three convolutional codes with code rates of $R = \frac{1}{3}$, $R = \frac{1}{2}$, and $R = \frac{2}{3}$ and a random interleaver ([29]). Without an error correction code, we observe that the proposed index mapping attains a negligible SNR gain over the conventional index mapping at the BER of 10^{-4}. By applying an error correction code, however, the gain of the proposed index mapping over the conventional index mapping tends to increase as the code rate decreases. We conclude that by applying an error correction code, the proposed index mapping can extract a substantial SNR gain over the conventional index mapping in various IM schemes such as OFDM-IQ-IM, CI-MM-OFDM-IM, and OFDM-IM.

In Fig. 11, the BER performances of classical OFDM, OFDM-IQ-IM with the proposed index mapping, and OFDM-IQ-IM with the equiprobable subcarrier activation (ESA) mapping ([22]) are compared in two cases of (a) $(n, k, p_1) = (8, 2, 4)$ and (b) $(n, k, p_1) = (8, 4, 5)$ with code rate $R = \frac{1}{2}$, when 4QAM is used for classical OFDM and binary PAM is used for the I- and Q- branches of OFDM-IQ-IM. From the figure, we observe that the proposed index mapping outperforms the ESA mapping in both the cases of $(n, k, p_1) = (8, 2, 4)$ and $(n, k, p_1) = (8, 4, 5)$.

Other simulation results not provided herein showed that the proposed index mapping and the ESA mapping yielded almost identical BER performance in the case of $(n, k, p_1) = (8, 3, 5)$ when 4QAM was used. Hereby, it can be summarized that while the SNR gain obtained by ESA mapping heavily depends on the number of active subcarriers given for a sub-block, the proposed index mapping can extract a considerable SNR gain for all the given values of the active subcarrier number.

VI. CONCLUSION

An index mapping algorithm that efficiently associates the ISB sequences with the SAP or CMP sequences was proposed. It was shown by numerical simulation that the proposed index mapping provided substantial performance improvement for various IM schemes such as OFDM-IQ-IM, CI-MM-OFDM-IM, and OFDM-IM, especially when an error correction code was applied simultaneously. An interesting future work is to expand the application of the proposed index mapping algorithm to various index modulation schemes with other transmission entities such as transmit antennas, time slots, etc.

APPENDIX

Herein, we prove that the i-th Gray-coded ISB sequence (i.e., $\mathbf{ISB}_i$) and the $(2^{p_1} - i + 1)$-th Gray-coded ISB sequence (i.e., $\mathbf{ISB}_{2^{p_1}-i+1}$) have Hamming distance 1. The number of the Gray-coded ISB sequences of length p_1 is 2^{p_1}. The binary sequence $\mathbf{B}_{2^{p_1}-i+1}$ can be obtained by complementing each element of $\mathbf{B}_i$, i.e.,

$$b_{2^{p_1}-i+1,l} = b_{i,l} \oplus 1 \quad \text{for } l = 1, 2, \cdots, n. \tag{43}$$

According to (23), $\mathbf{ISB}_i$ and $\mathbf{ISB}_{2^{p_1}-i+1}$ for $i = 1, 2, \cdots, 2^{p_1}$ can be written as

$$\mathbf{ISB}_i = [\, d_{i,p_1}\ d_{i,p_1-1}\ \cdots\ d_{i,1}\,] \tag{44}$$

and

$$\mathbf{ISB}_{2^{p_1}-i+1} = [\, d_{2^{p_1}-i+1,p_1}\ d_{2^{p_1}-i+1,p_1-1}\ \cdots\ d_{2^{p_1}-i+1,1}\,], \tag{45}$$

respectively. From (24), it follows that

$$d_{2^{p_1}-i+1,l} = \begin{cases} b_{2^{p_1}-i+1,l} & \text{if } l = p_1 \\ b_{2^{p_1}-i+1,l} \oplus b_{2^{p_1}-i+1,l+1} & \text{if } l = 1, \cdots, p_1 - 1 \end{cases} \tag{46}$$

for $i = 1, 2, \cdots, 2^{p_1}$. Based on (43), the expression of $d_{2^{p_1}-i+1,l}$ in (46) can be rewritten as

$$d_{2^{p_1}-i+1,l} = \begin{cases} b_{i,l} \oplus 1 & \text{if } l = p_1 \\ b_{i,l} \oplus b_{i,l+1} & \text{if } l = 1, \cdots, p_1 - 1, \end{cases} \tag{47}$$

where the identity of $(b_{i,l} \oplus 1) \oplus (b_{i,l+1} \oplus 1) = b_{i,l} \oplus b_{i,l+1}$ was used. Since $d_{i,p_1} = b_{i,p_1}$ and $d_{i,l} = b_{i,l} \oplus b_{i,l+1}$ for $l = 1, 2, \cdots, p_1 - 1$ as given in (24), it follows from (47) that

$$d_{2^{p_1}-i+1,l} = \begin{cases} d_{i,l} \oplus 1 & \text{if } l = p_1 \\ d_{i,l} & \text{if } l = 1, 2, \cdots, p_1 - 1 \end{cases} \tag{48}$$

for $i = 1, 2, \cdots, 2^{p_1}$. Therefore, from (44), (45), and (48), it is easy to see that the Hamming distance between $\mathbf{ISB}_i$ and $\mathbf{ISB}_{2^{p_1}-i+1}$ is given by 1.

REFERENCES

[1] E. Basar, M. Wen, R. Mesleh, M. Di Renzo, Y. Xiao, and H. Haas, "Index modulation techniques for next-generation wireless networks," *IEEE Access*, vol. 5, pp. 16693–16746, 2017.

[2] M. Wen, B. Zheng, K. Kim, M. D. Renzo, T. A. Tsitsis, K. Chen, and N. Al-Dhahir, "A survey on spatial modulation in emerging wireless systems: Research progresses and applications," *IEEE J. Sel. Areas Commun.*, vol. 37, no. 9, pp. 1949–1972, Sep. 2019.

[3] T. Mao, Q. Wang, Z. Wang, and S. Chen, "Novel index modulation techniques: A survey," *IEEE Commun. Surveys Tuts.*, vol. 21, no. 1, pp. 315–348, 1st Quart., 2019.

[4] P. K. Frenger and N. A. B. Svensson, "Parallel combinatory OFDM signaling," *IEEE Trans. Commun.*, vol. 47, no. 4, pp. 558–567, Apr. 1999.

[5] N. Ishikawa, S. Sugiura, and L. Hanzo, "Subcarrier-index modulation aided OFDM—Will it work?" *IEEE Access*, vol. 4, pp. 2580–2593, 2016.

[6] E. Ba ar, U. Aygölü, E. Panayırcı, and H. V. Poor, "Orthogonal frequency division multiplexing with index modulation," *IEEE Trans. Signal Process.*, vol. 61, no. 22, pp. 5536–5549, Nov. 2013.

[7] R. Fan, Y. J. Yu, and Y. L. Guan, "Orthogonal frequency division multiplexing with generalized index modulation," in *Proc. IEEE Global Commun. Conf. (GLOBECOM)*, Austin, TX, USA, Dec. 2014, pp. 3880–3885.

[8] R. Fan, Y. J. Yu, and Y. L. Guan, "Generalization of orthogonal frequency division multiplexing with index modulation," *IEEE Trans. Wireless Commun.*, vol. 14, no. 10, pp. 5350–5359, Oct. 2015.

[9] M. Wen, B. Ye, E. Basar, Q. Li, and F. Ji, "Enhanced orthogonal frequency division multiplexing with index modulation," *IEEE Trans. Wireless Commun.*, vol. 16, no. 7, pp. 4786–4801, Jul. 2017.

[10] Q. Li, M. Wen, E. Basar, H. V. Poor, B. Zheng, and F. Chen, "Diversity enhancing multiple-mode OFDM with index modulation," *IEEE Trans. Commun.*, vol. 66, no. 8, pp. 3653–3666, Aug. 2018.

[11] T. Mao, Z. Wang, Q. Wang, S. Chen, and L. Hanzo, "Dual-mode index modulation aided OFDM," *IEEE Access*, vol. 5, pp. 50–60, 2017.

[12] T. Mao, Q. Wang, and Z. Wang, "Generalized dual-mode index modulation aided OFDM," *IEEE Commun. Lett.*, vol. 21, no. 4, pp. 761–764, Apr. 2017.

[13] M. Wen, E. Basar, Q. Li, B. Zheng, and M. Zhang, "Multiple-mode orthogonal frequency division multiplexing with index modulation," *IEEE Trans. Commun.*, vol. 65, no. 9, pp. 3892–3906, Sep. 2017.

[14] J. Li, S. Dang, M. Wen, X. Jiang, Y. Peng, and H. Hai, "Layered orthogonal frequency division multiplexing with index modulation," *IEEE Syst. J.*, vol. 13, no. 4, pp. 3793–3802, Dec. 2019.

[15] Y. Xiao, S. Wang, L. Dan, X. Lei, P. Yang, and W. Xian, "OFDM with interleaved subcarrier-index modulation," *IEEE Commun. Lett.*, vol. 18, no. 8, pp. 1447–1450, Aug. 2014.

[16] E. Ba ar, "OFDM with index modulation using coordinate interleaving," *IEEE Wireless Commun. Lett.*, vol. 4, no. 4, pp. 381–384, Aug. 2015.

[17] Y. Liu, F. Ji, H. Yu, F. Chen, D. Wan, and B. Zheng, "Enhanced coordinate interleaved OFDM with index modulation," *IEEE Access*, vol. 5, pp. 27504–27513, 2017.

[18] M. Wen, Q. Li, E. Basar, and W. Zhang, "Generalized multiple-mode OFDM with index modulation," *IEEE Trans. Wireless Commun.*, vol. 17, no. 10, pp. 6531–6543, Oct. 2018.

[19] M. Wen, Y. Zhang, J. Li, E. Basar, and F. Chen, "Equiprobable subcarrier activation method for OFDM with index modulation," *IEEE Commun. Lett.*, vol. 20, no. 12, pp. 2386–2389, Dec. 2016.

[20] S. Dang, G. Chen, and J. P. Coon, "Lexicographic codebook design for OFDM with index modulation," *IEEE Trans. Wireless Commun.*, vol. 17, no. 12, pp. 8373–8387, Dec. 2018.

[21] S. Dang, G. Ma, B. Shihada, and M.-S. Alouini, "Enhanced orthogonal frequency-division multiplexing with subcarrier number modulation," *IEEE Internet Things J.*, vol. 6, no. 5, pp. 7907–7920, Oct. 2019.

[22] J. Li, M. Wen, X. Cheng, Y. Yan, S. Song, and M. Lee, "Differential spatial modulation with gray coded antenna activation order," *IEEE Commun. Lett.*, vol. 20, no. 6, pp. 1100–1103, Jun. 2016.

[23] X. Li, H. Wang, N. Guan, and W. Lai, "A dual-mode index modulation scheme with Gray-coded pairwise index mapping," *IEEE Commun. Lett.*, vol. 22, no. 8, pp. 1580–1583, Aug. 2018.

[24] F. Gray, "Pulse code communication," U.S. Patent 2 632 058 A, Nov. 13, 1947.
[25] J. Kim and E. Yoon, "Subcarrier segmentation based index mapping for OFDM index modulation," *J. KICS*, vol. 44, no. 2, pp. 199–207, Mar. 2019.
[26] I. M. Onyszchuk, "Truncation length for Viterbi decoding," *IEEE Trans. Commun.*, vol. 39, no. 7, pp. 1023–1026, Jul. 1991.
[27] *LTE Evolved Universal Terrestrial Radio Access (E-UTRA): Multiplexing and Channel Coding, Version 10.0.0 Release 10*, document ETSI TS 36.212, 3GPP, Jan. 2011.
[28] S. Bawane and V. V. Gohokar, "Simulation of convolutional encoder," *Int. J. Res. Eng. Technol.*, vol. 3, no. 3, pp. 557–561, Mar. 2014.
[29] L. Ping, L. Liu, K. Y. Wu, and W. K. Leung, "On interleave-division multiple-access," in *Proc. IEEE Int. Conf. Commun.*, Jun. 2004, pp. 2869–2873.

EUNCHUL YOON received the B.S. and M.S. degrees in electronics engineering from Yonsei University, Seoul, South Korea, in 1993 and 1995, respectively, and the Ph.D. degree in electrical engineering from Stanford University, CA, USA, in 2005. From February 1995 to July 2000, he was with the Samsung CDMA System Development Team, Seoul, where he was involved in the design of system software. From December 2005 to February 2008, he was with the Samsung WiMAX System Development Group, Suwon, South Korea, where he developed the modem methods for beamforming and MIMO. He has been with the Department of Electrical and Electronics Engineering, Konkuk University, Seoul, since March 2008. His research interests include wireless networks, coding and modulation, interference cancelation, and deep learning for wireless communications.

SUN-YONG KIM received the B.S.E. *(summa cum laude)*, M.S.E., and Ph.D. degrees in electrical engineering from the Korea Advanced Institute of Science and Technology (KAIST), Daejeon, in 1990, 1993, and 1995, respectively. From April 1995 to March 1996, he was a Visiting Researcher at The University of Tokyo, Tokyo, Japan. From March 1996 to August 2001, he was with the Department of Electronics Engineering, Hallym University. He joined the Department of Electrical and Electronics Engineering, Konkuk University, in September 2001, where he is currently a Professor. His research interests include detection and estimation theory, statistical signal processing, and the analysis and design of mobile communication systems.

He received the Second-Best Paper Award from the IEEE Korea Section in 1990, a scholarship from the IEEE Communication Society from 1992 to 1993, and a Paper Award from the LG Information and Communications, in 1994.

SOONBUM KWON is currently pursuing the bachelor's degree with the Department of Electrical and Electronics Engineering, Konkuk University, Seoul, South Korea. His research interests include wireless networks, coding and modulation, interference cancelation, and deep learning for wireless communications.

UNIL YUN received the M.S. degree in computer science and engineering from Korea University, Seoul, South Korea, in 1997, and the Ph.D. degree in computer science from Texas A&M University, Texas, USA, in 2005. He worked at the Multimedia Laboratory, Korea Telecom, from 1997 to 2002. He worked as a Postdoctoral Associate for almost one year at the Computer Science Department, Texas A&M University. Then, he worked as a Senior Researcher with the Electronics and Telecommunications Research Institute (ETRI). In March 2007, he joined the School of Electrical and Computer Engineering, Chungbuk National University, South Korea. Since August 2013, he has been with the Department of Computer Engineering, Sejong University, Seoul, South Korea. His research interests include data mining, information retrieval, database systems, artificial intelligence, and digital libraries.